# Coherent control of metallic nanoparticles near fields: Nanopulse controllers and functional nanoamplifiers

S. M. Sadeghi*
*Department of Physics, University of Alabama in Huntsville, Huntsville, Alabama 35899, USA*
(Received 16 January 2010; revised manuscript received 18 May 2010; published 12 July 2010)

When a hybrid system consisting of a metallic nanoparticle and a semiconductor quantum dot interacts with a coherent light source (laser beam) the coherence generated in the quantum dot can significantly renormalize the plasmonic field. In this paper we study the impacts of such coherent-plasmonic processes when such a hybrid system interacts with amplitude-modulated laser fields. We demonstrate how such these processes allow the metallic nanoparticle to act as a nanoamplifier and a pulse controller for the quantum dot. We show that as a nanopulse controller the metallic nanoparticle can control the shapes of optical pulses experienced by the quantum dot, including dramatic modification of their widths. As a functional nanoamplifier the metallic nanoparticle can enhance high intensity parts of a pulse train while suppressing the parts that their intensities are less than a given value. Therefore, it not only can enhance the amplitudes of the optical pulses but also can make them return-to-zero pulses.

DOI: 10.1103/PhysRevB.82.035413 PACS number(s): 73.21.La, 78.67.Hc, 85.35.Be

## I. INTRODUCTION

Currently one of the cornerstones of research in nanophotonics is investigation of the impacts of metallic nanoparticles or localized surface-plasmon resonances (LSPRs) on the optical properties of semiconductor nanostructures. This is an important field of research with significant applications, ranging from fundamental research in controlling emission of semiconductor nanoscrytals to the development of chemical and biological nanosensors,[1–4] electrical DNA switches, and nanodevices.[5] Many of these studies have been implemented in heterogeneous hybrid systems consisting of metallic nanoparticles (MNPs) and semiconductor quantum dots (QDs). These studies have already attracted significant attentions for colorimetric sensing,[6] detection of energy transfer between nanoparticles, construction of active nanostructures,[7] and enhancement of Forster energy transfer.[8,9]

One of the main foundations of the above studies is the electric field enhancement induced by LSPRs.[3,4] This process, although short range, is one of the main links between MNPs and their diverse and ground-breaking applications in various fields. Despite this, however, currently the main perception is that the plasmonic field enhancement experienced by QDs in QD-MNP hybrid systems is mostly the prime property of the MNPs and is not influenced by the QDs.[3,4] This assumption is not always valid, however. In fact when a QD-MNP system interacts with a coherent light source (laser field) the plasmonic field of the MNP can be renormalized significantly by the QD. In other words, the QD can dramatically influence the plasmonic field and, therefore, renormalizes the field that it feels. The main reason for this is the fact that the interaction of the QD with a laser beam generates coherence in the QD. Through dipole-dipole coupling such coherence influences the internal field of the MNP and, therefore, renormalizes the plasmon field. One of the main consequences of such coherent-plasmonic processes is to allow hybrid systems consisting of MNPs and QDs to have molecularlike resonances, called plasmonic metaresonances (PMRs).[10] Such resonances are related to the time delay induced by such processes in the response of a QD when it interacts with a time-dependent optical field.[11] PMR refers to the event wherein the environmental conditions of the QD-MNP systems (such as refractive index) or the distance between the QDs and MNPs reach a critical point causing this delay to become infinite. Since such a process strongly depends on the environments of the hybrid systems, it can have numerous applications, including chemical, biological, and physical sensors.

The objective of this paper is to show how coherent-plasmonic processes can be used to control modulation and amplification of optical fields interacting with QDs. We demonstrate that these processes allow MNPs to act as nanopulse controllers and functional nanoamplifiers. As nanoamplifiers MNPs not only allow us to use coherent-plasmonic processes to enhance the optical field experienced by the QDs significantly but also to suppress the background light between the pulses, making them return-to-zero pulses. As nanopulse controllers we show that by putting a MNP in the vicinity of a QD we can control the optical pulse shapes that the QD experiences. In particular, by bringing a MNP close to a QD the optical pulses experienced by the QD can become significantly narrower. Detailed discussions of the theory and the physics behind these phenomena will be discussed.

## II. COHERENT-PLASMONIC CONTROL OF PLASMONIC FIELDS

The core objective of this study is inclusion of coherent-plasmonic processes in the dynamics of QDs when they are in the vicinity of MNPs and are exposed to an amplitude-modulated single-mode laser field. This field drives plasmons in the MNP and excitons in the QD. Considering these two excitations as two dipole moments, the resultant field experienced by the QD is combination of three terms: (i) the external field, (ii) the field formed by direct excitation of plasmon by the laser field, and (iii) the field that is generated by the QD itself via excitation of the plasmons. (iii) relates to

 

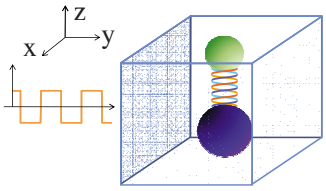


FIG. 1. (Color online) Schematic illustration of a unit of nanoamplifier/nanopulse controller studied in this paper. The incoming optical field is amplitude modulated with a polarization along the $z$ axis. The QD and MNP are put in the vicinity of each other with a distance of $R$ via a spacer or linker.

the fact that the electric dipole of the QD generates a field in the MNP and then the MNP in turn generates a field in the QD. This is basically the main essence of the coherent-plasmonic processes since the third term is induced via generation of coherence in the QD by the laser field.

A unit of the nanoamplifier/nanopulse controller studied in this paper is shown in Fig. 1. It consists of a spherical Au MNP with a radius $a$ and a QD separated from the MNP by the distance $R$. Such a system can be formed using, for example, biological conjugation of these two nanoparticles using polypeptides,[2,12] DNA,[13] antibody-mediated bioassembly,[7] etc. We consider the environment holding this system has permittivity $\varepsilon_0=1.8$, such as water. The interaction between the QD and the MNP is characterized by the large electric dipole moments of the QD and plasmon resonance of the MNP. Since the MNP has nanoscale dimension, its interaction with the laser field is treated within quasistatic approximation. The dielectric function of the MNP, $\varepsilon_m$, includes contributions of both $d$ electrons ($\varepsilon^d$) and the Drude contributions ($\varepsilon^s$). The former is obtained considering the real and imaginary parts of the interband permittivity of Au (Ref. 14) while the latter is given by

$$\varepsilon^s(\omega) = 1 - \frac{\omega_p^2}{\omega[\omega - i\Gamma(a)]}, \tag{1}$$

where $\Gamma(a)=\Gamma_\infty - Av_f/a$ refers to the damping parameter including surface-scattering mean-free-path effect. For the Au MNPs studied in this paper we considered $A=1$ and $\Gamma_\infty=0.1$ eV.[14,15] Additionally $\omega_p$ and $v_f$ in the above equation refer, respectively, to the plasmon frequency and Fermi velocity of Au.[14]

To describe how much the field experienced by the QD is enhanced by the plasmonic effects we usually define an enhancement factor. Conventionally this parameter depends on $R$, MNP specifications, and the matrix or environment.[3,4] The issue can become dramatically different when coherent-plasmonic effects are included, i.e., the QD-MNP system interacts with a coherent light source (a laser field). In fact considering these effects, the field intensity experienced by the QD ($I$) can be written as

$$I = P_i(\omega, I_0) I_0. \tag{2}$$

Here

$$P_i(\omega, I_0) = \frac{|E_i^{cp}(\omega, I_0)|^2}{|E_i^q|^2} \tag{3}$$

refers to the electric field enhancement factor when the laser field is polarized along $i$ ($i=x$, $y$, and $z$), $I_0$ to the intensity of the applied laser field and $\omega$ to the frequency of this field. Here $E_i^{cp}$ and $E_i^q$ refer, respectively, to the amplitude of the electric field of the laser beam in the presence and absence of the MNP. As highlighted clearly in Eq. (3) here the amplitude of the field experienced by the QD in the presence of the MNP ($E_i^{cp}$) now depends on the frequency and intensity of the applied field. These are the characteristics of the coherent-plasmonic effects which allow the QD renormalizes its own field. As will be shown in the following in the presence of the MNP $E_i^{cp}$ depends on the coherence that is generated in the QD by the laser field. Obviously if one considers incoherent light sources to excite the hybrid system, coherence is not generated in the QD and Eq. (3) becomes identical to what has already been investigated.[3,4]

To elaborate more on Eqs. (2) and (3) and to see how one can control the plasmonic near field of MNPs via QDs, consider the applied laser field interacting with the hybrid system is polarized along the $z$ axis $[E^q=E_z^q(t)\cos(\omega t)]$, as shown in Fig. 1. Considering these issues interaction of the QD with MNP and the laser field can be described by the following equation:

$$\frac{\partial \rho}{\partial t} = -\frac{i}{\hbar}[H(\rho), \rho] + \left.\frac{\partial \rho}{\partial t}\right|_{\text{relax}}. \tag{4}$$

Here $\rho$ refers to the density matrix of the QD system, and the second term represents the relaxation term of the QD that is not influenced by the presence of the MNP. In fact this term illustrates the energy relaxation and dephasing rates of the excitons, considered to be 1/0.8 and 2.7 $\text{ns}^{-1}$.[16,17] $H(\rho)=H_0+W_{\text{int}}(\rho)$, wherein $H_0$ refers to the Hamiltonian of the system in the absence of the laser field, and $W_{\text{int}}(\rho)$ represents the interaction term of the QD with this field in the presence of the MNP. Note that $W_{\text{int}}$ depends on the solution of Eq. (4) via the exciton-plasmon coupling. Within rotating wave and dipole approximations this term is given by

$$W_{\text{int}}(\rho) = \hbar\Omega_{12}^r(\rho) c_2^\dagger c_1 + \hbar\Omega_{12}^{r*}(\rho) c_1^\dagger c_2, \tag{5}$$

where $c_i^\dagger$ and $c_i$ refer, respectively, to the creation and annihilation operators of $|i\rangle$ with $i=1$ and 2 representing the ground and upper states of the fundamental exciton transition of the QD (the 1–2 transition). $\Omega_{12}^r$ is the normalized Rabi frequency given by[11]

$$\Omega_{12}^r(\rho) = \Omega_{eff} - i\frac{1}{\tau_F}\rho_{21} - \text{Re}\left[\frac{4\gamma\mu_{12}^2}{\hbar\varepsilon_{eff1}^2}\frac{a^3}{R^6}\right]\rho_{21}. \tag{6}$$

Here $\varepsilon_{eff1}=\frac{(2\varepsilon_0+\varepsilon_s)}{3\varepsilon_0}$, $\varepsilon_s$ refers to the dielectric constant of the QD, and $\rho_{21}$ represents the slowly varying part of the coherence generated by the laser field in the QD. $\mu_{12}$ is the dipole moment associated with the 1–2 transition and $\gamma=\frac{\varepsilon_m(\omega)-\varepsilon_0}{\varepsilon_m(\omega)+2\varepsilon_0}$. $\Omega_{eff}=\Omega_{12}^0(1+\frac{2\gamma a^3}{R^3})$ and $\Omega_{12}^0=-\frac{\mu_{12}E_0(t)}{2\hbar\varepsilon_{eff1}}$ refers to the Rabi frequency when the QD is isolated (very large $R$). $\frac{1}{\tau_F}$ represents

the Forster energy-transfer rate from the QD to the MNP given by

$$\frac{1}{\tau_F} = \mathrm{Im}\left[\frac{4\gamma\mu_{12}^2}{\hbar\varepsilon_{eff1}^2}\frac{a^3}{R^6}\right]. \tag{7}$$

Considering these issues, the equation of motion for $\delta=\rho_{22}-\rho_{11}$ and $\rho_{21}$ are obtained as follows:

$$\frac{\partial\delta}{\partial t} = 4\ \mathrm{Im}[\Omega_{12}^r\rho_{21}] + \left.\frac{\partial\delta}{\partial t}\right|_{\mathrm{relax}}, \tag{8}$$

$$\frac{\partial\rho_{21}}{\partial t} = -[i\Delta_{eff} + \gamma_{21} + \Xi_{\mathrm{relax}}^{\mathrm{plas}}]\rho_{21} - i\Omega_{eff}\delta. \tag{9}$$

Here

$$\Delta_{eff} = \Delta_{21} - \mathrm{Re}\left[\frac{4\gamma\mu_{12}^2}{\hbar\varepsilon_{eff1}^2}\frac{a^3}{R^6}\right]\delta \tag{10}$$

and $\Xi_{\mathrm{relax}}^{\mathrm{plas}} = \frac{1}{\tau_F}\delta$. $\Delta_{21}$ refers to the detuning of the applied optical field from the 1–2 transition in the absence of the plasmonic effects (large $R$). In the following we consider $\Delta_{21}=0$.

Considering the above equations the coherent-plasmonic field-enhancement factor [Eq. (3)] can be calculated using

$$P_z(\omega,I_0) = \left|\frac{\Omega_{12}^r(\rho)}{\Omega_{12}^{(0)}}\right|^2. \tag{11}$$

This equation clearly indicates that in contrast to previous studies,[1,4] when coherent-plasmonic effects are included the enhancement factor depends on the frequency and intensity of the exciting field. To obtain $\Omega_{12}^r(\rho)$ we solved Eqs. (8) and (9) including time-dependent variation in the applied field amplitude.[11] Additionally, Eq. (11) is consistent with Eq. (3) considering

$$E_z^{cp} = -\Omega_{12}^r\left(\frac{2\hbar\varepsilon_{eff1}}{\mu_{12}}\right). \tag{12}$$

Considering Eq. (6), this equation demonstrates how the amplitude of the field experienced by the QD depends on its own coherence and Forster energy transfer. In the following sections we show how by just changing the MNP size ($a$) and the energy of the QD transition we can apply the formalism described in this section to the cases representing coherent nanoamplifiers and nanopulse controller.

## III. COHERENT NANOAMPLIFIERS

To study the significance of the QD coherence in the near fields of LSPRs, in Fig. 2 we show how $P(\omega,I_0)$ changes with $R$ for different intensities of the laser field ($I_0$). We assumed this laser is resonant with the fundamental exciton transition of the QD (the 1–2 transition) and its photon energy ($\hbar\omega$) is 2.28 eV. We also here consider $a=14$ nm. This figure shows that when the QD and MNP are far from each other (large $R$) $P(\omega,I_0)$ is basically equal to unity, i.e., no significant field enhancement occurs. As $R$ reduces, however, depending on the intensity of applied field, $P(\omega,I_0)$ can be very different. For high-field intensities ($I_0=128$ W/cm$^2$) the enhancement factor monotonously increases (dots). This is basically what has been shown previously considering only plasmonic effects.[3,4] For smaller field intensities, however, the scenario becomes completely different. In fact for $I_0=2.8$ W/cm$^2$, after some slight increase and reaching a peak, $P(\omega,I_0)$ drops significantly as $R$ decreases further (squares). For $R=26$ nm, the amount of enhancement becomes insignificant. For $I_0=8$ W/cm$^2$ the enhancement factor reaches its peak at smaller $R$ with a higher amplitude (circles). It decreases, however, more abruptly as $R$ becomes smaller.

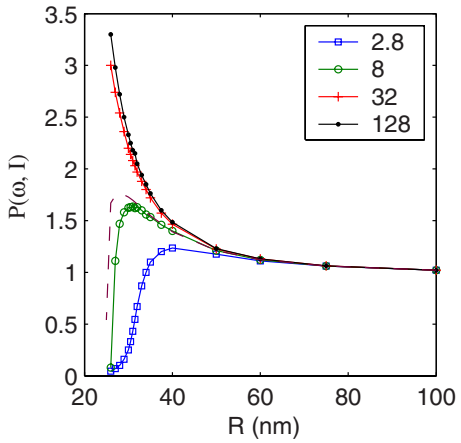


FIG. 2. (Color online) Variation in $P(\omega,I_0)$ with $R$ for different values of applied field intensities, $I_0$ (numbers in legends in W/cm$^2$). The dashed line represents the case of $I_0=8$ W/cm$^2$ when the Forster energy-transfer rate is turned off.

Note that the results shown in Fig. 2 are rather unique. They encompass two main features, which are not accommodated in the previous investigations of plasmonic field enhancement. The first feature is that $P(\omega,I_0)$ can be influenced by Forster energy transfer from the QD to the MNP, and the second feature is the impact of PMR. The abrupt decline of enhancement factor seen in Fig. 2 as $R$ reduces is the sign of PMR. When this phenomenon happens the field experienced by the QD is screened dramatically and, therefore, $P(\omega,I_0)$ becomes insignificant. PMR is quite well pronounced for the case of $I_0=8$ W/cm$^2$ and to less degree in the case of $I_0=2.8$ W/cm$^2$. Much sharper drops happen for $I_0=32$ and 128 W/cm$^2$ but that requires smaller $R$'s that considered in Fig. 2. Note that conventional methods that do not consider this effect predict monotonous increase in the enhancement factor as $R$ reduces, in contrast to what seen in Fig. 2.[3,4] Additionally, in this paper PMR is studied in a quasisteady-state condition, i.e., at times well after the turn on process of the laser field. In Ref. 10, however, this process was studied in time domain, wherein one can see the combined effects of coherent and plasmonic effects can delay response of a QD to a time-dependent optical field. When $R$ reaches a critical value this delay becomes infinite, i.e., PMR happens and the field experienced by the QD is screened strongly at all times. PMR is different from conventional transitions such as those happen between energy states of atoms, molecules, etc., via an optical field. Rather it corresponds to transition between

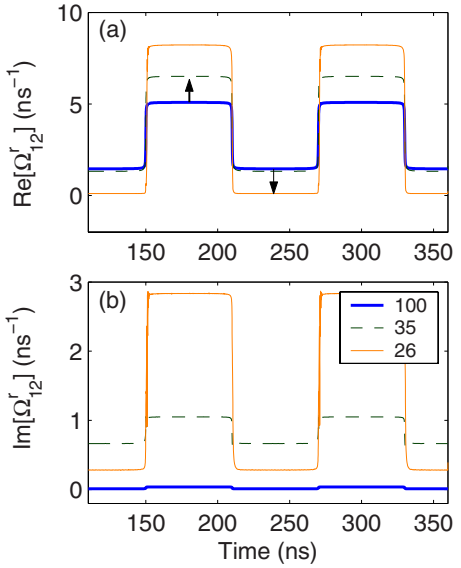


FIG. 3. (Color online) Variation in the (a) real and (b) imaginary parts of $\Omega_{12}^r$ with time for different values of $R$ (legends in nanometer). The thick line in (a) also represents $\Omega_{12}^0$, indicating the form of the applied field. Here $a=14$ nm, $\varepsilon_0=1.8$, and the 1–2 transition energy is 2.28 eV.

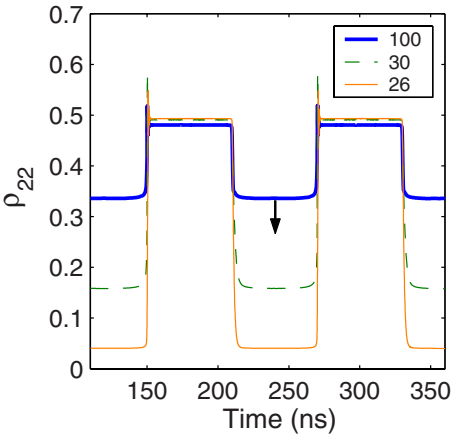


FIG. 4. (Color online) Variation in $\rho_{22}$ in the QD as a function of time for different values of $R$ (legends in nanometer). All other specifications are the same as those in Fig. 3.

two states of a QD-MNP system with significantly different forms of exciton-plasmon coupling.

Moreover, the results shown in Fig. 2 show that $P(\omega, I_0)$ is also influenced by the Forster energy transfer between the QD and the MNP. To see this note that one of the prime impact of this process is to make the 1–2 transition broadened as $R$ reduces. Such a broadening influences interaction of the laser field with the QD and, therefore, changes the enhancement factor. To clarify this we artificially turned off the Forster energy transfer for the case when $I_0=8$ W/cm$^2$. The dashed line in Fig. 2 shows that this increases the strength of the interaction of the laser field with the system, as if the intensity of applied laser field was higher. This was expected since broadening reduces the impact of laser field on the QD.

The results presented in Fig. 2 form the core foundations of the nanoamplifiers introduced in this paper. As mentioned in Sec. I, such amplifiers are not just about amplifying the near field experienced by the QD via plasmons. Rather, here we consider coherent-plasmonic effects which, as shown in Fig. 2, can be dramatically different from the pure plasmonic effects. A significant feature of the nanoamplifiers studied in this section is the fact that they are functional. This means that we can set the performance of these amplifiers, acting as linear amplifiers that amplify all parts of a pulse train, i.e., the minima and maxima, or adjust them such that they enhance the maxima while reducing the minima to nearly zero.

To start we consider a train of identical optical pulses reaching a unit of the QD-MNP system, as shown in Fig. 1. We consider this system is identical to the one considered in Fig. 2. To see how such a system allows the MNP to act as a functional nanoamplifier, in Fig. 3 we show variations in the (a) real and (b) imaginary parts of $\Omega_{12}^r$ as $R$ is changed. For $R=100$ nm the optical pulses experienced by the QD are very similar to the applied pulses. Therefore, since under this condition $\Omega_{12}^r=\Omega_{12}^0$, the thick line in Fig. 3(a) shows nearly the form of the applied field. This shows that the maximum intensity of the applied field is 32 W/cm$^2$(Re$[\Omega_{12}^r]$ $=5$ ns$^{-1}$) and the minimum (trough) intensity is 2.8 W/cm$^2$(Re$[\Omega_{12}^r]=1.5$ ns$^{-1}$). As $R$ decreases, however, one can see $\Omega_{12}^r$ becomes complex while the intensities of the maxima are increased and the trough intensities are decreased. For $R=26$ nm (thin solid lines), the maxima of real and imaginary parts of $\Omega_{12}^r$ reach 8.2 and 2.8 ns$^{-1}$. This corresponds to a field intensity of more than 100 W/cm$^2$. On the other hand, the trough intensities of the pulse train become nearly zero. These results suggest amplification as well as formation of a zero state in the pulse train, forming return-to-zero pulses.

To study the impact of variation in the normalized Rabi frequency on the population, in Fig. 4 we show the corresponding results for $\rho_{22}$. Here one can see that for $R=100$ nm, when the coherent-plasmon effects are ignorable, $\rho_{22}$ varies between 0.48 and 0.34 (thick line). With the decrease in $R$ the maxima go as far as they can (0.5) while the minima are decreased dramatically (thin line). For $R=26$ nm, the values of the latter become significantly small (0.04). Therefore, these results suggest significant increase in the extension ratio in the population oscillation. The overshoots seen in this figure are associated with Rabi flopping.[11]

## IV. COHERENT NANOPULSE CONTROLLERS

The results represented in the preceding section showed enhancement and suppression of the peak and trough intensities of an optical pulse without causing any significant pulse-shape deformation. Two main features that contributed to these were the energy of the QD and the size of the MNP. It is well known that as MNPs become larger they can lead to larger enhancement factors for QDs.[3,4] Also, as clarified in the next section, for a given MNP the enhancement factor is maximum when the QD transition frequency is slightly less than that of the plasmon peak.[3,4] For these reasons in the preceding section for the refractive index considered for the

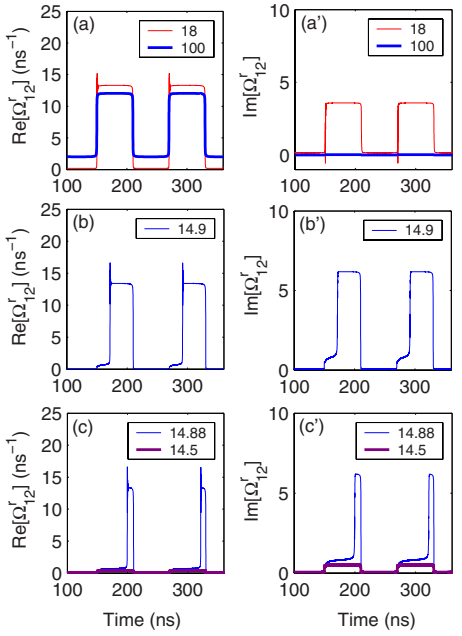


FIG. 5. (Color online) Variation in the real (a), (b), and (c) and imaginary (a′), (b′), and (c′) parts of $\Omega_{12}^r$ with time for different values of $R$ (legends in nanometer). The thick line in (a) also represents $\Omega_{12}^0$, indicating the form of the applied field. Here $a=7$ nm, $\varepsilon_0=1.8$, and the 1–2 transition energy is 2.37 eV.

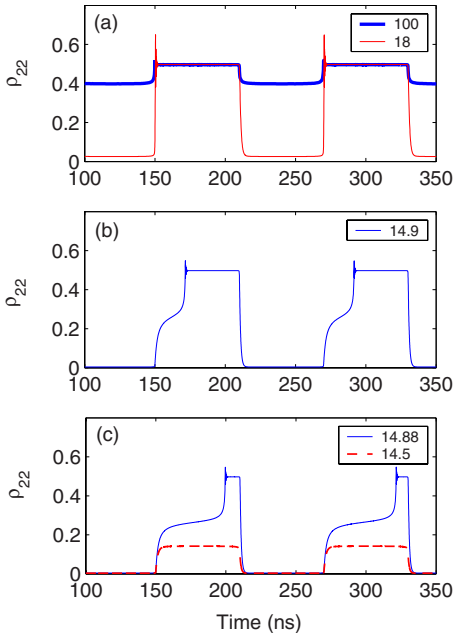


FIG. 6. (Color online) Variation in $\rho_{22}$ for corresponding cases considered in Fig. 5.

environment and $a=14$ nm we found the maximum enhancement factor happened when the 1–2 transition energy became equal to 2.28 eV. Obviously larger MNPs could be more beneficial in this sense but this weakens dipole approximation considered in this paper.

To study nanopulse controllers we need to consider a situation wherein the shapes of the optical pulses can be changed dramatically. For this, we utilize the mechanism responsible for formation of PMR, i.e., time delay in the response of a QD to a time-dependent optical field via coherent-plasmonic effects.[10] This requires setting up a strong dynamic normalization of the damping and detuning of the 1–2 transition and exciton excitation as the QD-MNP interacts with the laser pulses. For this we need to consider conditions where $\Xi_{\text{relax}}^{\text{plas}}$ and $\Delta_{\text{eff}}$ [Eqs. (8) and (9)] are changed significantly with time as the QD-MNP interacts with the optical pulses. Therefore, they can strongly renormalize such interaction, changing the shapes of the effective fields experienced by the QD considerably. As clarified in the following and discussed in Sec. V, we found the main criterion for having nanopulse controller is to have large Forster energy-transfer rate $(\frac{1}{\tau_F})$. For this reason in this section we consider the QD transition energy is 2.37 eV, i.e., the energy wherein $\frac{1}{\tau_F}$ becomes maximum. We also need to reduce $R$ as much as possible. This is rather more convenient for smaller MNPs since we can decrease $R$ considerably without getting too much close to the MNP. For this reason in this section we consider $a=7$ nm while considering other parameters are the same as those in the preceding section.

To study how a MNP can act as a coherent pulse controller, in Fig. 5 we study variation in the real and imaginary parts of $\Omega_{12}^r$ as $R$ is changed. Figure 5(a) show that when $R$ is large, the field experienced by the QD has the same form as the applied field (thick line). For $R=18$ nm, similar to the cases shown in Fig. 3, the coherent-plasmonic effects increase the maxima of the pulse train and reduce its minima [Fig. 5(a), thin line]. With further decrease in $R$ the effective optical pulses are changed in dramatic ways. As shown in Figs. 5(b) and 5(c), with a slight reduction in $R$ the widths of the optical pulses are reduced significantly. When $R=14.5$ nm, nearly the whole optical pulses are washed away and only some residual remain [Fig. 5(c), thick line]. Figures 5(a′)–5(c′) show the corresponding variation in imaginary part of the normalized Rabi frequency.

The results of calculations shown in Fig. 5 show that the shapes of the optical pulses experienced by the QD can be dramatically different from those of the applied optical field. To determine the impacts of these on the carrier excitation in the QD, in Fig. 6 we show how $\rho_{22}$ changes with $R$ under the same conditions as those in Fig. 5. Here we can see when $R$ is large $\rho_{22}\sim 0.5$ or 0.4 (thick line). For $R=18$ nm, the minima become very close to zero while the maxima remain fairly unchanged [Fig. 6(a)]. Note also that here with the reduction in $R$ the overshoots become more significant. This is because of the fact that under this condition the carriers are pushed from a state with nearly zero field to high field, resulting more significant Rabi oscillation.[11] With further decrease in $R$, as seen in Figs. 6(b) and 6(c), the population is exited in two steps, one from zero to about 0.25 and the other from 0.25 to 0.5. The second step becomes narrower with further decrease in $R$. When $R$ passes a limit the whole excitation process is suppressed (dashed line). These show that the carrier excitation is dramatically influenced by the coherent-plasmonic processes and can be controlled to a large extent.

In terms of polarization of the QD the system studied in Fig. 5 is quit intriguing. To see this in Fig. 7, we show the

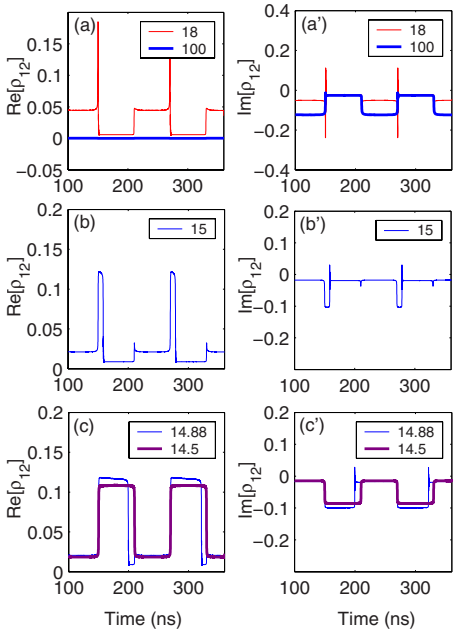


FIG. 7. (Color online) Variation in the real of imaginary parts of $\rho_{12}$ for the corresponding cases considered in Fig. 5.

corresponding dynamics of the real and imaginary parts of $\rho_{12}$ for the same values of $R$ as those in Fig. 5. Here one can see for very large $R$, Re$[\rho_{12}]$ is nearly zero and Im$[\rho_{12}]$ is rather large [thick lines, Figs. 7(a) and 7(a′)]. This means that the QD under this condition is quite absorptive at the maxima of the pulse train. As $R$ decreases, however, spikes of Re$[\rho_{12}]$ and Im$[\rho_{12}]$ are generated. As $R$ reduces the width of such spikes are increased. In other words, $\rho_{12}$ evolves in opposite to $\Omega_{12}^r$. For $R=14.5$ nm [thick lines, Figs. 7(c) and 7(c′)], under the condition where $\Omega_{12}^r$ is significantly screened, Re$[\rho_{12}]$ and Im$[\rho_{12}]$ form trains of pulses with significant maxima. Note that, similar to Fig. 6, the results presented in Fig. 7 were obtained when $\hbar\omega=2.37$ eV.

## V. DISCUSSION

As mentioned above the primary reason for pulse narrowing seen in Fig. 5 is the fact that coherent-plasmonic effects can induce time delay in the response of the QD to a time-dependent optical field. To clarify this issue and the physics behind nanopulse controllers discussed in the preceding section note that $\Xi_{\text{relax}}^{\text{plas}}$ and $\Delta_{eff}$ not only depend on Forster energy-transfer rate and the detuning caused by the plasmonic effects but also on $\delta$. Therefore, damping, detuning, and carrier excitations of the 1–2 transition can dynamically influence each other. When the optical field is weak and $R$ is small, $\delta\sim 1$ and both $\Delta_{eff}$ and $\Xi_{\text{relax}}^{\text{plas}}$ are large. This suggests that, although we consider the applied optical field is resonant with the 1–2 transition when $R$ is large ($\Delta_{21}=0$), for weak-field intensities and small $R$ it becomes detuned from this transition ($\Delta_{eff}\neq 0$). It also means that this transition can become dramatically broadened, if $\frac{1}{\tau_F}$ is large. When the optical field becomes strong and $\delta\sim 0$, however, both $\Delta_{eff}$ and $\Xi_{\text{relax}}^{\text{plas}}$ become insignificant. Considering the fact that large

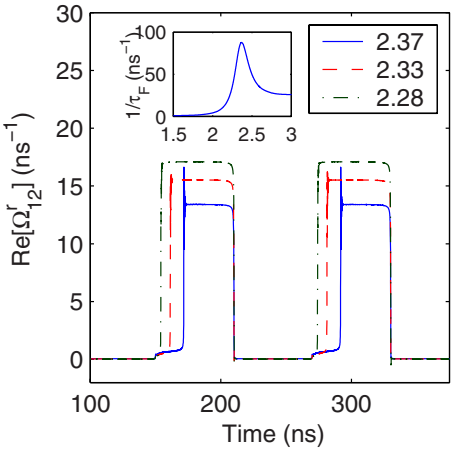


FIG. 8. (Color online) Variation in the real part of $\Omega_{21}^r$ with time for variation energies of the 1–2 transition (legends in electron volt). The inset shows $\frac{1}{\tau_F}$ as a function of this energy ($x$ axis in electron volt). Other conditions are the same as those in Fig. 5(b).

broadening and detuning hinder interaction of a laser field with the QD, when the optical field is weak plasmonic effects make the system more resistant against such interaction, causing delay in the optical excitation and reduction in $\delta$. Therefore, around the rise times of the applied optical pulses the field experienced by the QD is screened. As the applied optical field becomes strong ultimately the mutual interaction between $\delta$ and $\Delta_{eff}$ and $\Xi_{\text{relax}}^{\text{plas}}$ may turn in favor of very small $\delta$ and, therefore, the field experienced by the QD reaches its plateau. This process, which led to the time delay seen in Fig. 5, is not repeated during the fall times of the optical pulses, as under this condition the system starts from $\delta\sim 0$. Note also that when the value of $R$ reaches a critical value where the amount of plasmonic shift and broadening become so extensive such that $\delta$ remains large at all time [dashed line, Fig. 6(c)] PMR happens.[10]

To discuss the role of Forster energy-transfer rate in nanopulse controllers in Fig. 8 we showed results of calculation for the same system as that in Fig. 5(b) but varied the 1–2 transition energies (QD size). The inset of Fig. 8 also shows variation in $\frac{1}{\tau_F}$ with energy (in eV), indicating its peak value at 2.37 eV and sharp decline for smaller energies. The results shown in Fig. 8 show that with the reduction in the 1–2 transition energy and, therefore, decrease in $\frac{1}{\tau_F}$, the amount of the pulse narrowing decreases and ultimately vanishes. Additionally, these results show that this process is accompanied with enhancement of the amplitude of the optical pulses. In fact the maximum peak is reached when this energy is equal to 2.28 eV. For energy less than 2.28 eV the amplitude starts to decrease. This explains why in the preceding section we consider the 1–2 transition equal to 2.28 eV.

Additionally the results presented in Secs. III and IV were obtained under the condition where $\Delta_{21}=0$, i.e., the laser field was resonant with the 1–2 transition when $R$ is large. The situation changes if one considers the cases where $\Delta_{21}$ is not zero. To show a typical example of sensitivity of the results to $\Delta_{12}$ in Fig. 9 we consider the system considered in Fig. 5(b) but varied $\Delta_{21}$. The results show that with the in-

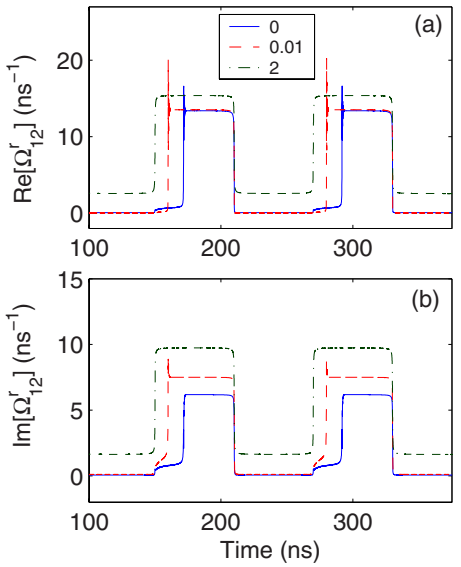


FIG. 9. (Color online) Variation in the real part of $\Omega^r_{21}$ with time for various detunings ($\Delta_{21}$) of the 1–2 transition (legends in millielectron volt). Other conditions are the same as those in Fig. 5(b).

crease in $\Delta_{21}$ the narrowed optical pulses become broadened, retaining their own original shapes. Changing the sign of $\Delta_{21}$ can lead to different amplitudes for the optical pulses since $\Omega^r_{12}$ can be frequency dependent.[11]

The results presented in Figs. 5–7 show high sensitivity to the distance between the MNP and QD ($R$). Regarding this issue note that, as mentioned in Sec. II, the MNPs studied in this paper were spherical and their interaction with the QDs was treated within dipole-dipole approximation. Therefore, $R$ represents the center-to-center distance between the nanoparticles. Under these conditions, one way to study the impact of variations in the size and geometry of the MNPs and QDs is to find out how they influence this approximation. Of course the more the QDs get closer to the MNPs variation in the time delay with respect to the system parameters, including size and shape variations, refractive index fluctuations, etc., become more dramatic. Therefore, although the pulse narrowing process still happens, its value with respect to $R$ becomes less certain. One way to have more control over the system is to reduce the intensity of the laser field. As shown in Fig. 2, this allows PMR happens at larger $R$. Therefore, the time delay required for the pulse narrowing can also be reached at larger $R$ and the results become less sensitive to local variations in the MNP shapes. Additionally, when applied optical pulses are narrower one can make significant relative changes in their temporal widths with smaller delays. This means that one can stay farther from PMR, wherein the delay is not very sensitive to $R$, and generate enough delay to cause relatively large changes in the optical pulses.

## VI. CONCLUSIONS

We showed that MNPs could act as nanodevices such as functional optical nanoamplifiers and pulse controllers for semiconductor QDs. For this, the MNPs need to be in the vicinity of QDs and both of them are exposed to a laser field. Via combined effects of plasmons in the MNPs and the coherence generated in the QDs, we demonstrated MNPs can enhance and trim optical pulses that the QDs experience. MNPs can also dramatically change the shapes of the optical pulses experienced by the QDs and narrow them dramatically. The physics behind such nanodevices are dynamical normalization of plasmonic fields and the QDs' linewidths and damping rates.

*seyed.sadeghi@uah.edu

[1] K. Matsuda, Y. Ito, and Y. Kanemitsu, Appl. Phys. Lett. **92**, 211911 (2008).
[2] T. Pons, I. L. Medintz, K. E. Sapsford, S. Higashiya, A. F. Grimes, D. S. English, and H. Mattoussi, Nano Lett. **7**, 3157 (2007).
[3] A. O. Govorov, G. W. Bryant, W. Zhang, T. Skeini, J. Lee, N. A. Kotov, J. M. Slocik, and R. R. Naik, Nano Lett. **6**, 984 (2006).
[4] A. O. Govorov and I. Carmeli, Nano Lett. **7**, 620 (2007).
[5] U. Rant, E. Pringsheim, W. Kaiser, K. Arinaga, J. Knezevic, M. Tornow, S. Fujita, N. Yokoyama, and G. Abstreiter, Nano Lett. **9**, 1290 (2009).
[6] L. Dyadyusha, H. Yin, S. Jaiswal, T. Brown, J. J. Baumberg, F. P. Booy, and T. Melvin, Chem. Commun. (Cambridge) **2005**, 3201.
[7] J. M. Slocik, A. O. Govorov, and R. R. Naik, Supramol. Chem. **18**, 415 (2006).
[8] A. O. Govorov, J. Lee, and N. A. Kotov, Phys. Rev. B **76**, 125308 (2007).
[9] V. K. Komarala, A. L. Bradley, Y. P. Rakovich, S. J. Byrne, Y. K. Gun'ko, and A. L. Rogach, Appl. Phys. Lett. **93**, 123102 (2008).
[10] S. M. Sadeghi, Phys. Rev. B **79**, 233309 (2009).
[11] S. M. Sadeghi, Nanotechnology **20**, 225401 (2009).
[12] I. L. Medintz, K. E. Sapsford, A. R. Clapp, T. Pons, S. Higashiya, J. T. Welch, and H. Mattoussi, J. Phys. Chem. B **110**, 10683 (2006).
[13] Y. Shan, J.-J. Xu, and H.-Y. Chen, Chem. Commun. (Cambridge) **2009**, 905.
[14] E. Cottancin, G. Celep, J. Lermé, M. Pellarin, J. R. Huntzinger, J. L. Vialle, and M. Broyer, Theor. Chem. Acc. **116**, 514 (2006).
[15] S. Link and M. A. El-Sayed, J. Phys. Chem. B **103**, 8410 (1999).
[16] W. Zhang, A. O. Govorov, and G. W. Bryant, Phys. Rev. Lett. **97**, 146804 (2006).
[17] R. D. Artuso and G. W. Bryant, Nano Lett. **8**, 2106 (2008).